Correction of Macroscopic Field Gradient Effect for Magnetic Field Correlation Imaging

K. U. Szulc[1], J. H. Jensen[1], H. Lu[1,2], L. Xuan[1], C. Hu[1], A. Ramani[1], M. F. Falangola[1,3], and J. A. Helpern[1,3]

[1]Center for Biomedical Imaging, Radiology, New York University School of Medicine, New York, NY, United States, [2]Advanced Imaging Research Center, University of Texas Southwestern Medical Center, Dallas, TX, United States, [3]Center for Advanced Brain Imaging, Nathan S. Kline Institute, Orangeburg, NY, United States

Introduction: Magnetic Field Correlation (MFC) is a recently introduced MRI measure that is sensitive to the microscopic magnetic field inhomogeneities generated in the brain by iron-rich tissue structures and provides information beyond that contained in more commonly used quantities for brain iron quantification, such as R2 and R2* [1-5]. Prior work indicates that the MFC increases rapidly during adolescence, consistent with known age-related brain iron changes [6] and that Alzheimer patients have elevated MFC values in the basal ganglia compared with age-matched controls [7]. Although these results support the usefulness of the MFC as an index of tissue iron, a possible confounding effect for the application of MFC imaging to the brain is the contribution of macroscopic field gradients to the MFC, in particular those generated by air cavities [4]. In this study, we propose a method for estimating the macroscopic contribution to the MFC ("macroMFC") from phase maps, which can be acquired with the same imaging protocol used for the total MFC and thus does not require an increase in the imaging time. We show that in several key regions of interest the macroMFC contributes 4 to 13% to the total MFC for a typical MFC imaging protocol.

Theory: MFC imaging is based on acquiring asymmetric spin echoes (ASE), as described in detail elsewhere [4], with the total MFC being derived from magnitude images. As is well known, phase images contain information about macroscopic (B_0) field variations and are often utilized to derive field maps [8]. This phase information can then be combined with the result,

$$\text{macroMFC} = \frac{\gamma^2}{12}\left(G_x^2 L_x^2 + G_y^2 L_y^2 + G_z^2 L_z^2\right) \qquad (1)$$

where γ is the proton gyromagnetic ratio, (G_x, G_y, G_z) are the macroscopic field gradients in the phase, read, and slice directions, and (L_x, L_y, L_z) are the corresponding voxel dimensions [4]. Thus, by deriving estimates for the macroscopic field gradients from the phase maps, the macroMFC can be determined.

Methods: 20 healthy subjects participated in the study (11 males, 9 females, mean age ± SD: 35 ± 10.1 years). Imaging was performed on a Siemens Trio 3T scanner. The MFC data were acquired using a segmented EPI ASE sequence with the 180º refocusing pulse shifted by a time t_s = 0, –4, –8, –12, and –16 ms from its standard position. Both the magnitude and phase images for each acquisition were saved. Other imaging parameters were: TR = 1500 ms, TE = 46 ms, FOV = 256 × 256 mm^2, bandwidth = 1346 Hz, EPI factor = 37, averages = 10, acquisition matrix = 192×192, slice thickness = 2 mm, interslice gap = 2 mm, and number of slices = 9. The MFC data were processed offline on a PC using in-house MATLAB scripts (Mathworks, Natick, MA). The parametric maps for the total MFC were derived from the magnitude images following an established method [4], while the macroMFC was derived from the phase maps by using finite differences to estimate the gradients and applying Eq. (1). Phase wrapping ambiguities were handled by determining the smallest possible gradient magnitudes consistent with the data, which is valid for gradients up to approximately 0.4 mT/m for our protocol.

Results and Discussion: A typical set of MFC images along with a corresponding anatomical image is given in Fig. 1. In the total MFC map (Fig. 1a), a significant macroMFC component is noticeable in the inferior frontal region of the brain presumably caused by the sinus air cavities. Subtracting the macroMFC map (Fig. 1b) from the total MFC maps yields a "microMFC" map (Fig. 1c) that more accurately reflects microscopic field inhomogeneities intrinsic to the tissue. As shown in Table 1, the average contributions of the macroscopic gradients to the MFC estimates were approximately 9% of the original MFC value and the fractional macroMFC contribution was found to be largest (13%) for frontal white matter and smallest (4%) for posterior white matter. Overall this study indicates that the macroscopic contributions to the MFC are modest and can be estimated and corrected. The correction may turn out particularly useful in early detection of iron imbalance associated diseases when the associated MFC changes may be small.

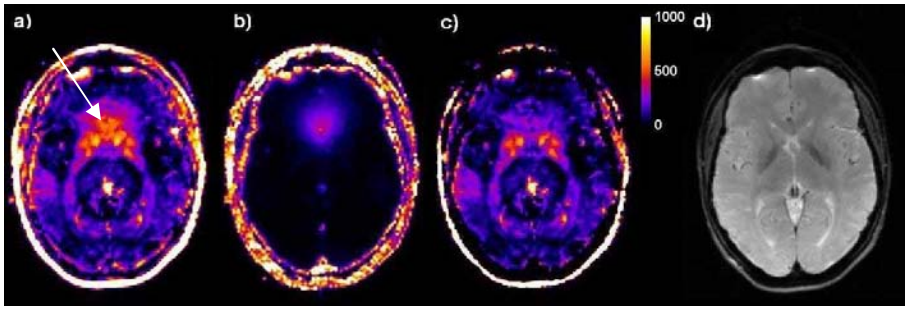

Figure 1. MFC images before and after correction for macroscopic gradients from a single subject: a) total MFC, b) macroMFC, c) microMFC, and d) corresponding anatomical image. Arrow in a) indicates a region of elevated MFC due to the sinus air cavity.

Region	MFC [s^{-2}]	macroMFC [s^{-2}]	microMFC [s^{-2}]	100 × macroMFC/MFC
GP	495 ± 26	35 ± 3	460 ± 25	7.0
PUT	301 ± 24	28 ± 3	274 ± 22	9.1
TH	97 ± 12	10 ± 1	87 ± 12	10.0
FWM	117 ± 8	15 ± 2	102 ± 7	12.7
PWM	127 ± 8	5.1 ± 0.2	122 ± 8	4.0
SPL	95 ± 8	8.7 ± 0.5	86 ± 9	9.3

Table 1. Regional MRI estimates (±SEM) for total MFC, macroMFC, microMFC, and the percent macroMFC to total MFC ratio. Regions reported are globus pallidus (GP), putamen (PUT), thalamus (TH), frontal white matter (FWM), posterior white matter (PWM) and splenium of the corpus callosum (SPL).

Acknowledgements: This work was supported in part by NIH grant R21/R33-EB003305, Werner Dannheisser Trust and the Litwin Fund for Alzheimer's Research.

References:

[1] Jensen JH, Chandra R. *ISMRM;* 10:2297 (2002), [2] Jensen JH, Johnson G, Chandra R, Helpern JA. *ISMRM;* 11:1120 (2003), [3] Ramani A, Jensen JH, Kaczynski K, Helpern JA, *ISMRM;* 13:2177 (2005), [4] Jensen JH, Chandra R, Ramani A, Lu H, Johnson G, Lee SP, Kaczynski K, Helpern JA. *MRM;* 55:1350-1361 (2006), [5] Lee SP, Falangola MF, Jensen JH, Lu H, Nixon RA, Duff K, Helpern JA. *ISMRM;* 14:975 (2006), [6] Ramani A, Jensen JH, Krain AL, Yang J, Hu C, Lu H, Helpern JA. *ISMRM;* 14:1559 (2006), [7] Ramani A, Szulc KU, Jensen JH, Lu H, Hu C, Ferris SH, Helpern JA. *ISMRM;* 14:2655 (2006), [8] Reber PJ, Wong EC, Buxton RB, Frank LR. *MRM;* 39:328-330.